Available online at www.CivileJournal.org

Civil Engineering Journal

Vol. 4, No. 12, December, 2018

Improving Flexural Behavior of Textile Reinforced Concrete One Way Slab by Removing Weft Yarns with Different Percentages

Omar H. Hussien [a*], Amer M. Ibrahim [a], Suhad M. Abd [a]

[a] *College of Engineering, University of Diyala, Baqubah, Diyala, Iraq.*

Received 13 September 2018; Accepted 11 December 2018

Abstract

Textile reinforced concrete that developed at recent years is composed of the continuous textile fabric incorporated into the cementitious matrix. The geometry of the textile reinforcements has a great influence on the TRC overall behavior since it affects the bond efficiency perfectly. The effect of weft yarns removing on the flexural behavior of (1500 × 500 × 50) mm one way slabs was investigated, eight layers of the carbon fabric were used with (50%, 67% and 75%) removing of weft yarns in addition to one specimen without removing. The four one- way slabs were casted by hand lay-up method, cured for (28) days and tested in flexure using four points method. The bending capacity and the bond efficiency factor were calculated according to the conditions of the equilibrium models by comparing with experimental results. The results revealed that with higher removing proportion there was a perfect improvement in the flexural capacity, higher first crack load, eminent post cracking stiffness, higher average concrete strain and lower ultimate mid span deflection and higher toughness and ductility. Furthermore, the results clarified that there is an optimum percent of weft yarns removing at which the damage occurrence around the weft yarns is significantly reduced, and this negative effect constriction overcome the positive anchoring effect.

Keywords: TRC; Weft Yarn Removing; One -Way Slab; Carbon Fabric; Hand Lay-Up.

1. Introduction

The brittleness nature of concrete with the slight tensile strength and low strain capacity promotes the demand for reinforcing with different reinforcements types. The textile reinforcements such as carbon, AR glass and Kevlar are mostly preferred in reinforcing concrete members as compared as compared with the other reinforcing materials due to their excellent properties in term of high tensile strength and modulus of elasticity. Moreover, premium ductility and non-corrosive nature are major characteristics for textile reinforcements when compared to short dispersed fibers and steel reinforcements, in addition, to their low weight to strength ratio, strain hardening behavior and yielding multiple micro cracks [1]. Furthermore, the flexible design possibility that the textile reinforcement exhibits considered a central characteristic made the use of such reinforcement materials is perfectly attractive [2].

The high performance fibers which are mentioned previously can be made up as filament, tows or yarns and fabric, used as a reinforcing material. The yarns or twos consists of many hundreds or thousands of continuous length (7-30) μm diameter filaments the external sleeve filaments are perfectly contact with the concrete matrix rather than the internal core filaments. Indeed, the actual percentage of the sleeve filaments which are in the direct contact with the matrix cannot be accurately evaluated for the reason of the complex micro structure of both textile and matrix. However, the number of filaments is inversely proportional with the bonding due to the penetration effect and the bond of single roving cannot indicate the bond of fabric in addition to the fabric geometry effect [3]. The sleeve filaments that represent

* Corresponding author: ekhel199276@gmail.com

http://dx.doi.org/10.28991/cej-03091207

(25%) of the total yarn filaments are quite strained under the tensile stresses whilst the residual core filaments are differently strained [4]. The bond efficiency is the major factor that controlled the mechanical behavior of the TRC structural member. The degree of concrete penetration through the yarns is perfectly controlling the bond efficiency while the external filaments which are in contact with the matrix play a vital role in TRCs manufacturing [5]. The bond efficiency can be improved by some casting techniques such as pultrusion process [6-8].

The geometry of the textile reinforcements considered one of the most influential factors that affect the TRC mechanical behavior since the interfacial bond between the textile reinforcements and the concrete matrix is quietly affected by fabric geometry. The congestion of the textile fabric in the concrete matrix has a double contrast effect on the bond efficiency, firstly, the congestion offers better mechanical anchoring that can enhance the bond of the yarn with the around matrix. While secondly, this congestion is significantly reducing the penetration of the matrix through the fabric openings. TRC members can be improved by eliminating the yarns at the direction transverse to the loading. Alrshoudi (2015) investigated the flexural behavior of the 500×100×100 mm beams that reinforced with 50 k filaments carbon textile reinforcements the obtained results showed that the ultimate load is improved with excluding whole weft yarns in the reason of reducing the reinforcement congestion which improves the penetration of the concrete matrix through the openings [9]. The weft yarns have a complex influence on the composite performance. Since the weft yarns anchor the longitudinal reinforcing yarns then restrain its sliding and the higher number of yarn junctions in the loading direction achieves further anchoring points. Despite that these weft yarns can promote the crack propagation and cause the delamination in the direction perpendicular to the loading. Therefore, the zones that near the weft yarns deemed weak points in the concrete matrix, high stress concentrations occur accompanied by cracks initiation and propagation in a sequential process. Furthermore, the weft yarns straighten under the tensile load effect during the test and causes severe damage near the junctions [10]. Peled et.al (1994, 1999) studied the effect of weft yarns removing on the flexural behavior of 10, 20 and 110 mm prisms reinforced by 22 warp yarn /cm monofilament polyethylene fabric with eight layers and 5.7% volumetric ratio with 5, 7, 10 yarns/cm at the transverse direction [11, 12].

The results clarified that the 7 fill yarns/cm fabric yield an optimal apparent flexural strength of 18 MPa as compared with the other 5 and 10 weft yarns that exhibited 15 and 13 MPa flexural strengths, respectively. The decreased flexural strength with the 10 weft yarns was attributed to the slight matrix compaction in addition to the weakening of the matrix by the fill yarns by defects function. On the other hand, the anchoring of the warp yarns by the fills and bond enhancement between the fabric and the matrix clarified the flexural strength difference between the 5 and 7 fill yarns specimens [10]. Figure 1 show the load deflection behavior for the three previous specimens. Colombo et al. (2013) investigated the tensile behavior of the specimens with 400, 70 and 6 mm in (long, width and thickness). The previous specimens were casted by hand lay-up with three several ways: (1) one AR-Glass fabric layer was placed between two concrete layers, (2) two fabric layers in a direct contact are placed between two concrete layers and (3) two fabric layers are separated by 2 mm concrete layer. The specimens reinforced with same warp yarns density while the weft yarns density was different according to the four 10, 20, 30, 50 mm spacing. The tensile test was carried out for all the specimens that obtained from the various production methods, a pressure of 3.9 and 5.6 MPa was applied to the specimen edges that glued by 3mm thick plates to achieve better distribution of the clamping pressure and to reduce the damage accompanied by local crushing. The results that obtained from the tensile tests were in terms of stress against normalized displacement as in Figures 2a and 2b. The specimens with the minimal fabric weft spacing yields lowest strength at the first crack about 3 MPa in the reason of tension stiffening reduction along the warp yarns. While the specimens with wider weft spacing showed the tension stiffening dominance with 7 MPa first crack strength. Furthermore, the presence of longer bond length leads to higher stiffness in the multi-cracking branch in both 30 and 50 mm since this effective bond length inhibits the longitudinal delamination. The 10 mm spacing specimens yield higher ultimate strain in the reason of intensive weft defect existence that achieve the roving stretching. Figure 2b showed the several patterns of cracking, disclosed cracks are observed between the weft yarns specially in 30 mm spacing specimen. However, the four different weft spacing specimens showed the same peak load [13].

Ghane and Lari (2014) developed a practical model to calculate the weft yarn deflection in the plain woven fabric by yarn pull-out test employment. The modelling was achieved by considering the weft yarn similar to an elastic beam, which is fixed at both ends and the middle deflection is imputed to the warp normal applied load. The weft yarns with the five various densities have been investigated. Four assumptions are applied to realize this weft yarn deflection model: (1) circular cross section of the yarns, (2) Elastic behavior of the yarns during bending, (3) the equations of small deflection are applied to the model and (4) the middle yarn point represents the position of vertical concentrated applied load. The (FK20) epoxy resin was used with the ratio (1:2) to impregnate the fabrics in a special mold, the 48 h curing process was stratified on the set of specimens and results a solid structure. The weft yarn maximum deflection was measured by applying microscopic photography on the fabric lateral cross section in order to compare with the theoretical deflection which is obtained from the small deflection equations that derived from the weft yarn curvature related to its bending rigidity. However, the bending rigidity calculation is realized from the bending rigidities relation between the fabric and thread. The results confirmed the perfect convergence between the actual weft yarn deflection curve and the theoretical model. However, the divergence between the two curve increased with the weft yarn density

reduction, this is imputed to diminish of the friction force by decreasing the weft yarn density, however, the friction force reduction at the both weft yarn ends constrict the fix supported assumption then leads to more divergence in theoretical model. In general, the deflection is directly proportional to the normal load while inversely proportional to the bending rigidity. Hence decreasing the weft yarn density reduce the normal force and decrease the bending rigidity while the maximum deflection is perfectly reduced and that confirmed the normal load domination. Moreover, the yarn flattening during weaving increased in weft direction particularly with higher densities however, this intense flattening reduces the bending rigidity [14]. Ortlepp (2018) stated that the reduction in the spacing between the cross yarns can improve the bond and reduce the development length in the coated textile reinforcements. An essential variation in the longitudinal fibers cross section created by cross fibers, this variation significantly occurs at the junctions. Furthermore, the glued cross and longitudinal fibers by the coating represents further anchorage zones that fixed the longitudinal fibers. However, increasing these anchorage zones leads to lower cross yarns spacing and slightly decrease the development length [15].

This work aims to investigate the optimum percentage of weft yarn removing at which the matrix weakening is reduced and the anchoring reduction effect is not perfectly occurring. This work studied the influence of weft yarns removing with the three different proportions on the bending capacity, average concrete strain, crack patterns and toughness and ductility of the three tested one way slabs while the fourth tested specimen is without removing in order to compare with the other three tested one-way slab specimens.

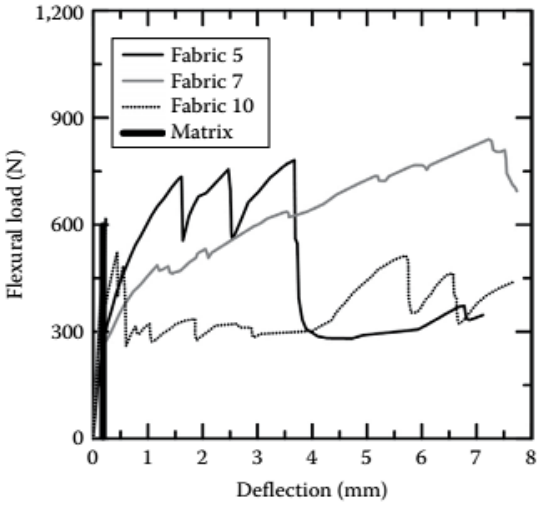

Figure 1. Flexural response of composites reinforced with fabrics made with different fill yarn densities perpendicular to the load direction (5, 7, and 10 fill yarns/cm). [12]

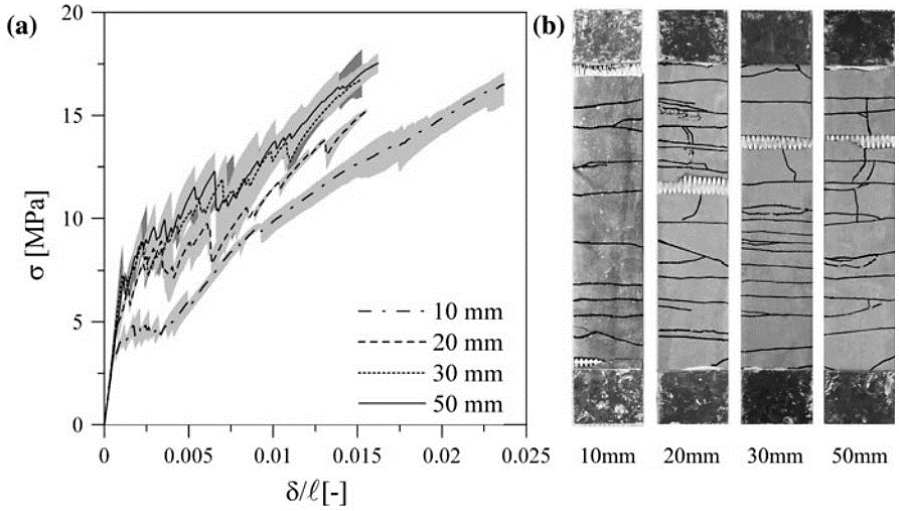

Figure 2. Influence of fabric geometry (different weft spacing) for a specimen reinforced with F3-1 fabric: (a) nominal stress versus normalized displacement curves in uniaxial tension and (b) specimen cracking pattern [13]

2. Methodology

2.1. Concrete Matrix

The concrete matrix that used in this study composed of the ordinary Portland cement, fine anti slip sand with grading

size 150-600 µm (see Figure 3), silica fume (micro silica), water and super plasticizer which is a hydrous solution of modified poly carboxylate basis. This product meets the requirements of (ASTM-C-494) [16]. Table 1 illustrates the matrix constituents and their quantities. The cylinder compressive strength 51 (standard deviation 6 MPa).

Table 1. Constituents of the fine grained concrete

Cement	**Kg/m^3**	650
Silica fume	**Kg/m^3**	50
Sand (0 - 0.6) mm	**Kg/m^3**	1215
Superplasticizer	**Kg/m^3**	15.3725
water	**Kg/m^3**	250
Cylinder compressive strength (28) day MPa		51
Flow ability, diameter in cm		25

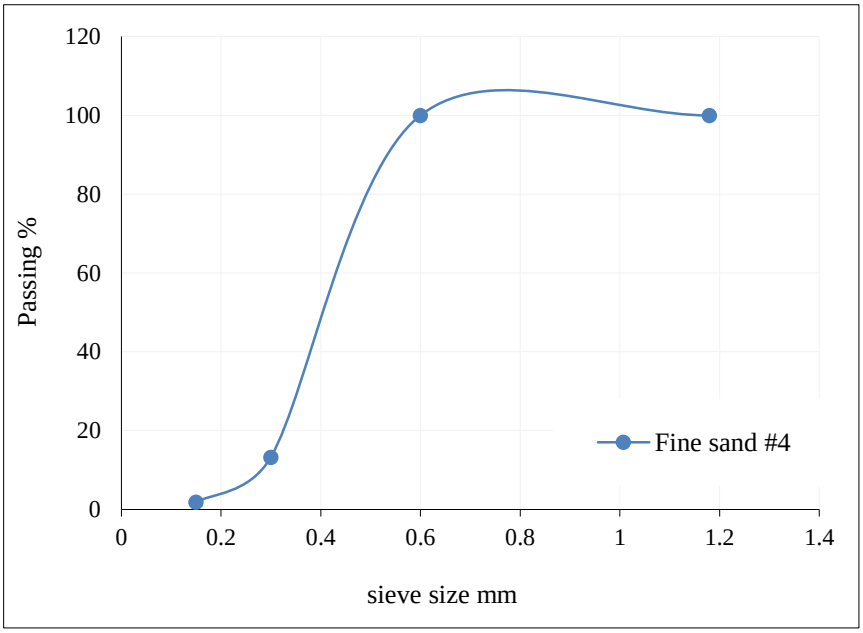

Figure 3. Grading curve of the Anti-slip sand #4

2.2. Textile Reinforcement Fabrics

One type of textile reinforcement is used in this study is the dry carbon fiber mesh (PAN) as shown in the Figures 4a and 4b with looping size of 2.5×3 cm and 12 k filament. This type of reinforcement was supplied from (JIAXING NEWTEX COMPOSITES), Table 2 shows the manufacturer data sheet, Figure 5 shows the reinforcements details for the one-way slab cross section. However, it must be mentioned that the tensile strength value of the carbon fabric that obtained from suppliers' data sheet is directly adopted without testing for the reason of un availability of an appropriate testing machine that acquire the accurate tensile test for the carbon fabric.

Table 2. Technical data sheet of carbon fabric

Material	12 k carbon fiber
Weight (g/m^2)	160 ± 10 (g)
Width (cm)	100
Thickness (mm)	0.2
Mesh size (cm)	2.5
Tensile strength (MPa)	3530
Tensile Modulus (GPa)	230
Color	Black

a) One layer in the play wood mold **b) Carbon fabric Roll**

Figure 4. Carbon fabric reinforcements

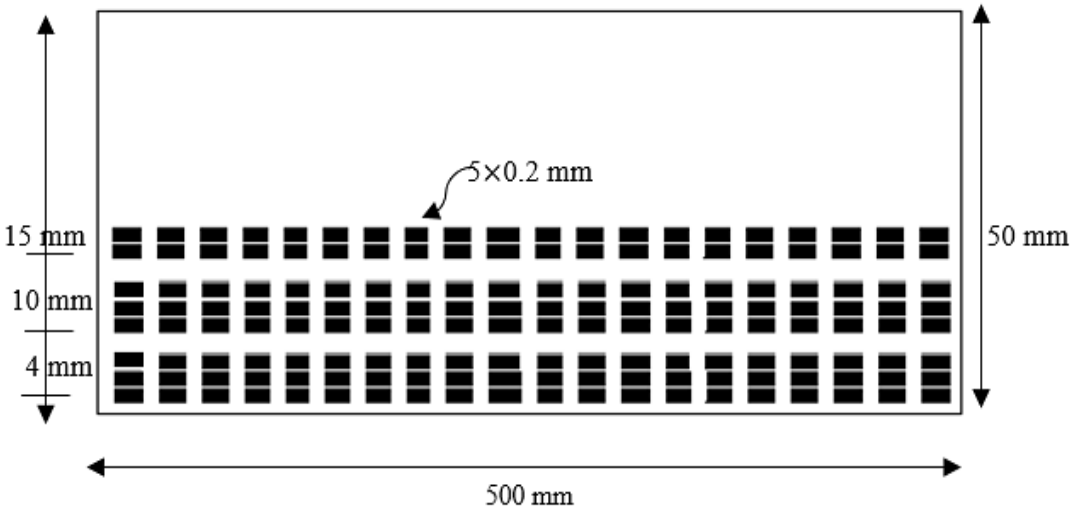

Figure 5. Reinforcement details for the specimen cross section

2.3. Sample Preparation

The play wood molds with dimensions of 1500 × 500 × 50 mm are used for casting the four one way slab specimens. Firstly the molds were oiled in order to inhibit the adhering of the concrete on the molds, the little amount of concrete is poured for 4 mm then the first three layers were sequentially placed with some squeezing for each layer applied by the hand levelling instrument to enhance the penetration of concrete matrix through the fabric openings. Particularly with 4 mm concrete cover and accumulation of fabric layers the delamination chance is increased hence this compaction method achieved to inhibit the delamination occurrence and to assure the fabric layers levelness. Another concrete amount is casted till 10 mm thickness where the second three layers were laid thereafter the last two layers were placed at the 15mm concrete thickness. The slight tension is applied by hands from the both opposite ends in order to keep the straightness and orientation of the layers. The specimens were demolded after 24 hours and cured for 28 days in a water curing basin with 23±2 ℃. The slab specimens were removed from curing after 28 days and dried, painted and fixed the strain gauges on its surfaces in order to perform the four-point bending test.

2.4. Instrumentation and Measurements

2.4.1. Deflection Measurement Devices

Three dial gauges were used to measure the vertical deflection (displacement) of the tested slab specimens. One was at the mid-span and the other two gauges were placed below each center of the distance between the support and the loading point. Hese dial gauges differentiate by their type, capacity and accuracy. The electronic dial gauge is with 25.4 mm capacity and 0.01 accuracy whilst the others are mechanical dial gauges with the capacity of 30-50 mm and accuracy of 0.01 mm. Figure 6a, 6b and 6c shows the dial gauge types. The deflection values that obtained from the three gauges were directly recorded for each applied load.


a) 30mm mechanical dial gauge **b) 1 in. electronic dial gauge** **c) 50 mm mechanical dial gauge**

Figures 6. Dial gauge types that used in this work

2.4.2. Strain Measurement Device

Strains were measured to determine the behavior of the one-way slab specimens against the applied stress. The use of highly accurate device is required to calculate the amount of strain in the concrete. The (BF120-20AA) strain gauge type that produced by SNC company was used to measure the compression strain of concrete during the test. Table 3 showed the properties of this strain gauge type and Figure 7 shows this strain gauge type.

Table 3. Strain gauge properties

Gauge Type	Resistance in Ω	Grid size (mm)	Gauge Dimensions	
			Length (mm)	Width (mm)
BF120-20AA	120	20×3.5	25	5

Figure 7. Strain gauge type that used in this work

The strain gauges were fixed on the concrete surface for each specimen and connected to the (TDS-530) data logger device (see Figure 8). The concrete strain values were saved and printed for each load.

Figure 8. (TDS-530) Data logger that used in this work

2.4.3. Crack Width Measurement Device

A micro-crack meter device was used to measure the cracks width. The crack meter that shown in Figure 9 is supplied by an adjustable light source and the power is provided by battery. This device can measure till 4 mm crack width with 0.02 mm division and 40x magnification factor used to measure the first crack width development at all stages of loading.

Figure 9. Micro-crack meter that used in this work

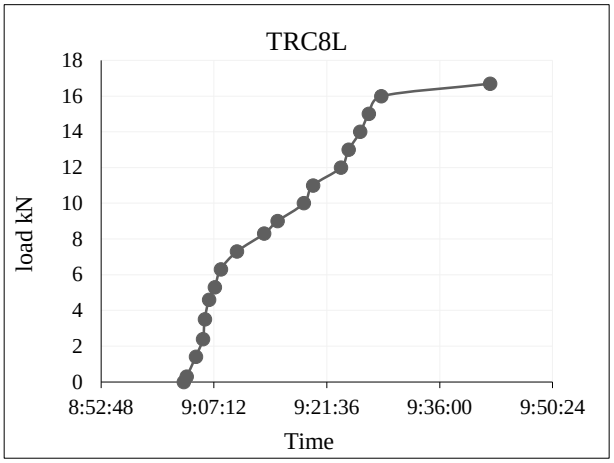

a. Load-Time curve for TRC 8L tested slab

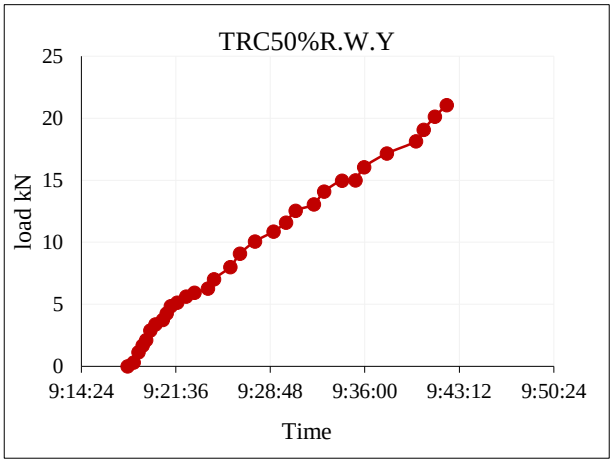

b. Load-Time curve for TRC 50 R.W.Y tested slab

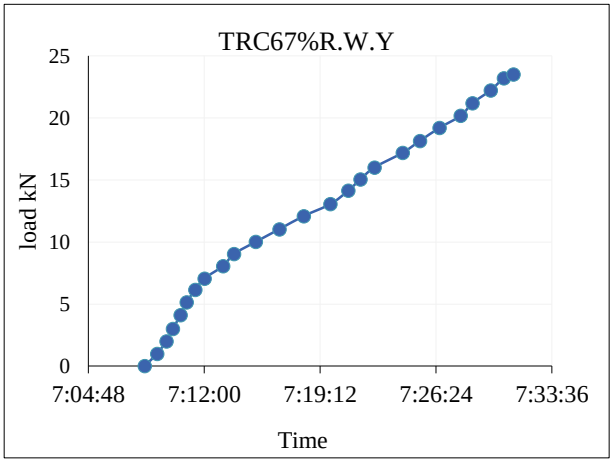

c. Load-Time curve for TRC 8L tested slab

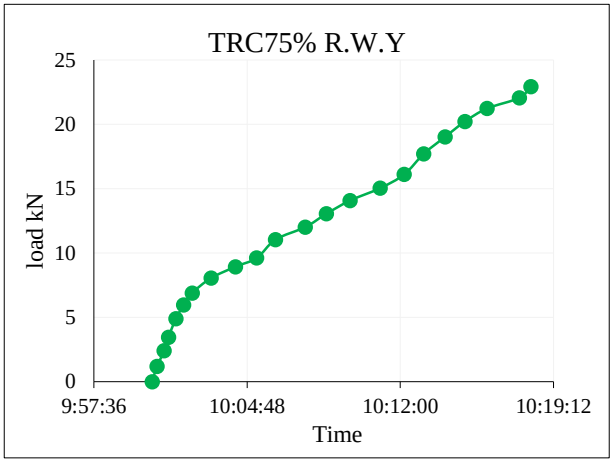

d. Load-Time curve for TRC 50 R.W.Y tested slab

Figures 10. Load-Time curve for the four tested one-way slabs

4. Results and Discussion

4.1. Bending Capacity of the Tested Slabs

Table 4 illustrates the first crack load, ultimate load and deflection of the four tested slabs. the results of the three removing tested slabs are compared with the (TRC 8L) results. From the table it can be noticed that the first crack load reduced by about 2.89% and increased by 13.68% and 14.24% for the (TRC 50% R.W.Y, TRC 67% R.W.Y and TRC 75% R.W.Y) respectively in comparison to the (TRC 8L). This can be demonstrated by the performance improvement

of the concrete matrix by enhance the penetration through the openings and the reduction of the discontinuity joints that caused by the weft yarns congestion. The ultimate flexural capacity increases gradually by about 20.65%, 28.94% and 27.23% for the (TRC 50% R.W.Y, TRC 67% R.W.Y and TRC 75% R.W.Y) respectively. This increase is attributed to the increase in the interfacial bond between the concrete matrix and the textile reinforcement. The bond efficiency factor increases by 21.51%, 30.52% and 28.66% for the (TRC 50% R.W.Y, TRC 67%R.W.Y and TRC 75% R.W.Y) respectively as compared to the (TRC 8L) bond efficiency. This is attributed to the better matrix penetration through mesh openings which improves the interfacial bond between the matrix and fabric. However, the effect of weft yarns mechanical anchoring was not observed, this might be for the reason of low slippage of the filaments since the yarn consists of low number of filaments as compared with 24 and 50 k yarns in addition to the matrix fineness that increases the matrix penetration chance through the yarn sleeve filaments then the friction perfectly occurs. The first crack stress and flexural strength as the two characteristic values were evaluated based on the idealistic linear behavior assumption despite that the actual magnitude and distribution of the stress are distinct concerning on material nonlinearity and depth of the crack, hence the apparent stress represents a modest measure for comparing various materials. Figure 11 shows the experimental first crack stress and ultimate flexural strength for the four tested slabs respectively. It can be noticed that the (TRC 75% R.W.Y and TRC 67% R.W.Y) yields the higher first crack stress and ultimate flexural strength respectively.

Table 4. The test results of the four tested slabs

Slab Symbol	% V_f	F.C load kN	UL load kN	Mid span Deflection mm	B. M kN.m	Bond factor η	Δ^+ Bond %
TRC 8L	0.528	5.3	16.7	46.34	4.593	0.478	–
TRC 50%R.W.Y	0.408	5.15	21.05	54.59	5.788	0.609	21.51
TRC 67%R.W.Y	0.368	6.14	23.5	43.52	6.07	0.688	30.52
TRC 75%R.W.Y	0.348	6.18	22.95	40.47	6.46	0.67	28.66

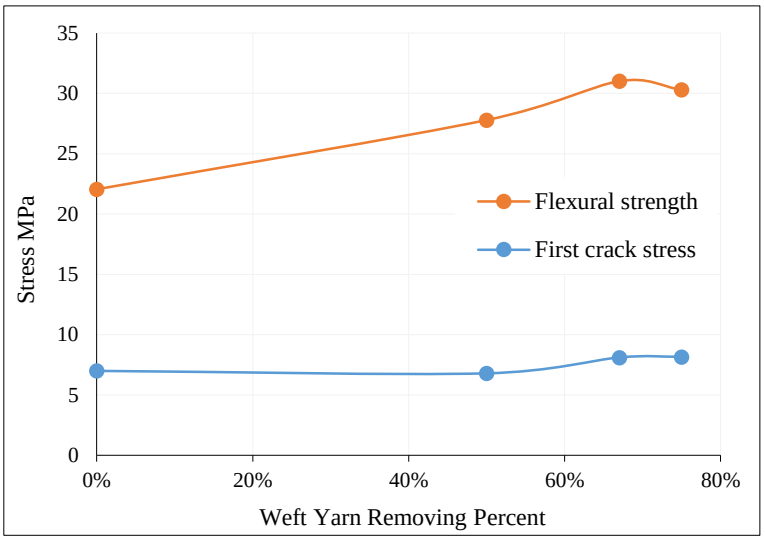

Figure 11. First crack and apparent flexural strength of the four tested slabs

4.2. Load-Deflection Behavior of the Tested Slabs

Figure 12 shows the deflection curves of the four tested slabs. From the previous table and the figure, it can be noticed that the deflection of the (TRC 50% R.W.Y) increased by about 15.11% as compared to the (TRC 8L) this can be attributed to the immediate deflection that is obtained after the formation of the first crack as its shown in the figure below that the deflection increases rapidly after the cracking with similar load intervals for that of the un cracked stage. This can be accounted to the possibility of low bond of one internal textile layer which is on the other hand increase the chance of core filaments slippage against the external filaments. However, the penetration of concrete is improved since the removing of the weft yarns increase the size of openings. The (TRC 67%R.W.Y and TRC 75% R.W.Y) shows reduction in the deflection by 6.09% and 12.67% respectively with respect to the ((TRC 8L). In spite the excess in the ultimate load in the two slab specimens. This can be imputed to the reduction in the slippage of the core filaments since the removing of the weft yarns enhance the matrix penetration and acquire the longitudinal bond improvement. Furthermore, the removing of the weft yarns with high proportions leads to reduce the curvature of the textile reinforcement layer itself since its with mesh shape then the concavity is diminished**.** It can be noticed that the (TRC

50% R.W.Y) is identical to the (TRC 8L) except the ultimate load and deflection. The (TRC 67%R.W.Y) shows the ascendant behavior in term of the lowest deflection for the highest load, (TRC 75% R.W.Y) on the other hand also shows small deflection with high load with respect to the two other slab specimens.

The load- mid span deflection curves can indicate the post cracking stiffness of each one way tested slab and as its observed the last two removing specimens shows the higher post cracking stiffness this is confirmed by the ultimate load accretion with the reduction in mid span deflection since the deflection of such structural member represents a function of loads, spans relative to member flexural stiffness. The post cracking stiffness is quite controlled by the textile reinforcements in such TRC members, however increasing the volume of textile fibers or its area is not necessary enhance the post cracking stiffness in contrary with the findings of Yin, Lü and Xu (2013) [17] who concluded that the un cracked stiffness of the TRC beam is not affect by increasing the number of textile layers whilst the post cracking stiffness can be improved by such increase whilst on contrast, Deju Zhu et al. (2017) concluded that the number of layers increasing is improving the bearing capacity of the TRC specimen while the slight reduction in the stiffness after the cracking is evident [18]. Indeed, increasing the area of textile reinforcements as a single factor may give this positive or negative effect on the post cracking stiffness since there is an essential other factor which is the bond efficiency factor that has a great effect on the post cracking stiffness. The bond efficiency is affected by the interfacial bond between the external filaments and concrete matrix since the latter has a significant influence on the stiffness after cracking rather than internal core filaments which yields marginal stiffness. The removing of the weft yarns with high percents improves the bond efficiency between the textile reinforcement and the cementitious matrix by increasing the penetration of the concrete matrix through the fabric openings hence the contribution of the core internal yarn filaments to the stiffness is increased.

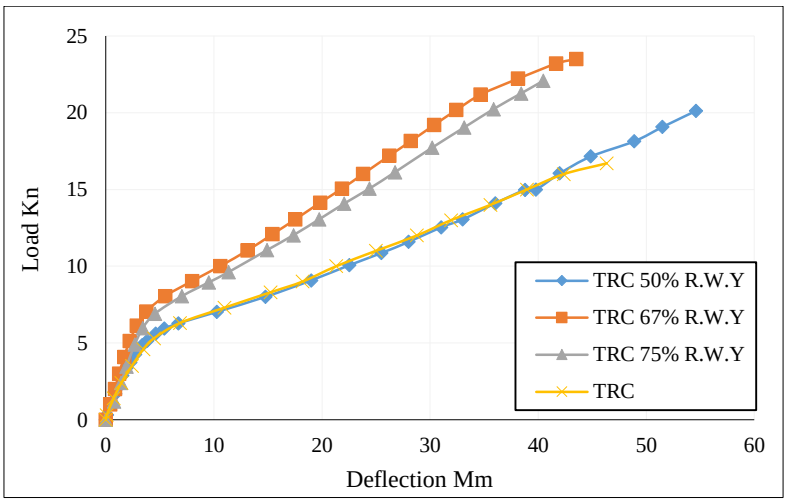

Figure 12. The load deflection behavior of the four tested slabs

4.3. Concrete Strain in the Compression Face

From the Table 5 it can be noticed that the top concrete strain at the first crack decreased in the three removing percent's specimens in comparison to the (TRC 8L) by about 7.5%, 24.59% and 18.97% for the (TRC 50% R.W.Y, TRC 67%R.W.Y and TRC 75% R.W.Y) respectively. This reduction can be attributed to the improvement in the matrix performance with continuous removing of weft yarns which increases the penetration of the matrix through the openings and on the other hand the matrix weakening zones that caused by the weft yarn accumulation are perfectly reduced with the removing of weft yarns then the intense damage is limited. The concrete strain in the compression zone for the four slab specimens in the post cracking stage is approximately double its values at the un cracked stage despite that the same intervals of load are applied during the two stages. The table also show that the ultimate strain is increased in the three percent's removing specimens as compared to the (TRC 8L) by about 18.11%, 11.3% and 1.35% for the (TRC 50% R.W.Y, TRC 67%R.W.Y and TRC 75% R.W.Y) respectively. This can be explained by the increasing in the compressive strength of the concrete matrix as a result from the concrete performance improvement.

Table 5. Compression concrete strain for the tested slabs

Slab symbol	Top face of concrete	
	$\varepsilon_{cr}\times10^{-6}$	$\varepsilon_{u}\times 10^{-6}$
TRC 8L	427	2188
TRC 50% R.W.Y	395	2672
TRC 67% R.W.Y	322	2467
TRC 75% R.W.Y	346	2218

Figure 13 demonstrates the load-compression concrete strain for the four tested slab specimens. The figure shows the linearity of the first un cracked stage for all specimens at which The concrete strain increases with the load increase by approximately constant increments. However, the second nonlinear stage shows the rapid strain accession with same load intervals of the previous stage. The identical pair (TRC 67%R.W.Y) and (TRC 75% R.W.Y) shows the lower concrete strain with the higher loads with respect to the other (TRC 50% R.W.Y) and (TRC 8L) identical pair.

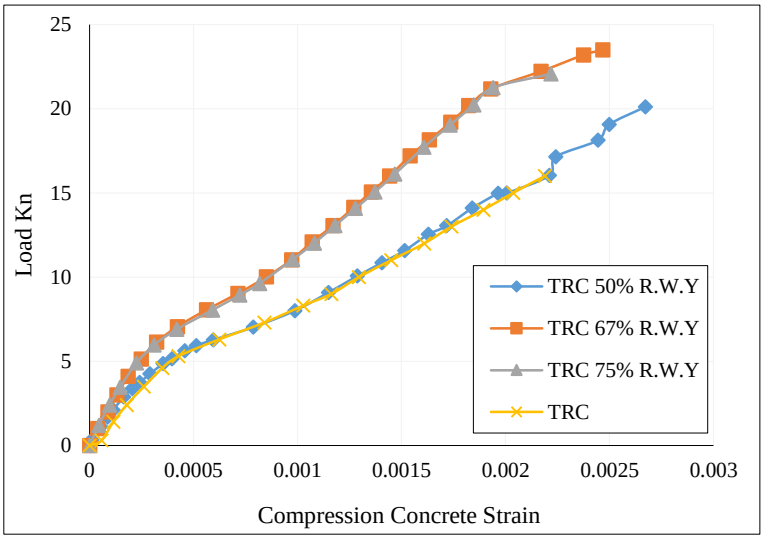

Figure 13. The load-average top concrete strain of the four tested slabs

4.4. Cracks Number, Width and Spacing of the Four Tested Slabs

The crack patterns are investigated in term of cracks number, width, spacing. The data were obtained from the four-point bending test. The crack was assigned with reading width by the crack micrometer and recorded for each applied load. Table 6 illustrates the cracks details of the four tested slab specimens. It can be observed that the first crack take place at about 31.74% of the ultimate load for the (TRC 8L) and at 24.45%, 26.13% and 26.93% for the (TRC 50% R.W.Y, TRC 67%R.W.Y and TRC 75% R.W.Y) respectively. This can be accounted to the increasing the ultimate strength capacity of the last three slabs. Despite that the first crack load is too increased particularly with the two higher removing specimens which is attributed to the effective tension stiffening that acquired in the longitudinal direction. The number of cracks is varying from one specimen to another. However, removing the across weft yarns is expected to minimize the cracks number and this is evidently occurring in the (TRC 50% R.W.Y and TRC 75% R.W.Y) when the cracks number reduced by 12.5% and 25% respectively. This reduction may attribute to the poor interfacial bond between the concrete matrix and some internal fabric layers in case of (TRC 50% R.W.Y) tested slab.

While the higher reduction in the textile mesh junctions at which the stresses concentrate. In addition to the matrix intense damage inhibition that occurs in the vicinity of the weft yarns leads to the lower number of cracks with the (TRC 75% R.W.Y). The horizontal cracks take place in case of (TRC 75% R.W.Y) specially at the main crack position in the reason of consecutive debonding existence with the longitudinal debonding inception that occurs in the yarn parallel to the load direction however this process is existed with the load accretion. On the other hand, (67% R.W.Y) shows the same number of cracks as compared to the (TRC 8L) this can be accounted to the high longitudinal interfacial bond between the matrix and the fabric mesh with eliminating of defeats which caused by the cross yarns. The effective tension stiffening is also improved by such bond enhancement. However, excluding the positive anchoring effect with this removing percent was not perfectly influenced the cracks initiation, propagation, numbers and width thus it can be considered an optimum percent of removing. The first crack width was the same for all tested one-way slabs however the width is only increased in the (TRC 50% R.W.Y) by about 20% as compared to the (TRC 8L) this can be attributed to the low stiffness that the (TRC 50% R.W.Y) yields beyond the first crack.

The textile reinforcements with the high modulus of Elasticity achieve the strain hardening and deflection hardening in both tensile and flexural tests respectively. In general, an excellent characteristic of the TRC with respect to the durability aspect which is the multiple cracking upon loading with the limiting crack width that not exceed (100 μm) [10]. The dense micro cracks are preferred in the behavior of the structural members rather than the few wider cracks. Figures 14a, 14b, 14c and 14d shows the cracks patterns for these tested slabs.

Table 6. Cracks patterns for the tested slabs

Slab symbol	First crack load kN	$\frac{\%\ F.C}{Pu}$	No. of cracks	Width of F. c mm	C. w @ ULs mm	Spacing cm		Mode of Failure
						Min	Max	
TRC 8L	5.3	31.74	40	0.02	0.1	1	3	F.F
TRC 50% R.W.Y	5.15	24.45	35	0.02	0.12	1	4.5	
TRC 67% R.W.Y	6.14	26.13	40	0.02	0.1	1	3	
TRC 75% R.W.Y	6.18	26.93	30	0.02	0.1	1	3	

a. The cracks pattern of the (TRC 8L)

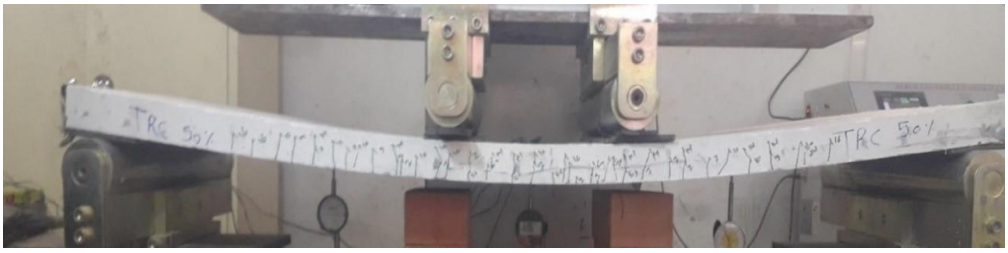

b. Cracks pattern of TRC 50% R.W.Y

c. Cracks pattern of TRC 67% R.W.Y

d. Cracks pattern of TRC 75% R.W.Y

Figure 14. Show the cracks patterns for the four tested one-way slabs

4.5 Toughness of the Four Tested TRC one, Way Slabs

Material toughness can be defined as the ability of energy absorbing beyond the rupture, however this stage known by the plastic stage. Toughness of the material can be evaluated from the load-deformation or stress-strain curves by calculating the total area under the curve relative to the specimen volume. the toughness of the four tested one way slabs is calculated by two methods. The first one is the numerical integration by Trapezoidal Rule (method 1) and the second is the integration of the curve equation which is obtained from the curve fitting in (Microsoft Excel) (method 2). The two methods are explained in the Figures 15a and 15b respectively and Table 7 illustrates the toughness for the overall tested slabs that calculated by the two methods with trivial relative difference that represents $((M2 - M1)/M1 \times 100\%)$.

Table 7. Toughness of the tested one, way slabs by two methods

Slab symbol	Member toughness (N.mm/mm³)			Difference Δ%
	Method 1	Method 2		
		$(\int_0^{\Delta u}$ 2nd.eq) / V	R^2	
TRC 8L	0.01284889	0.01272952	0.9735	-0.938
TRC50%R.W.Y	0.01693798	0.016736827	0.974	-1.202
TRC67%R.W.Y	0.01724498	0.017115307	0.9812	-0.758
TRC75%R.W.Y	0.01425497	0.014191464	0.9799	-0.447

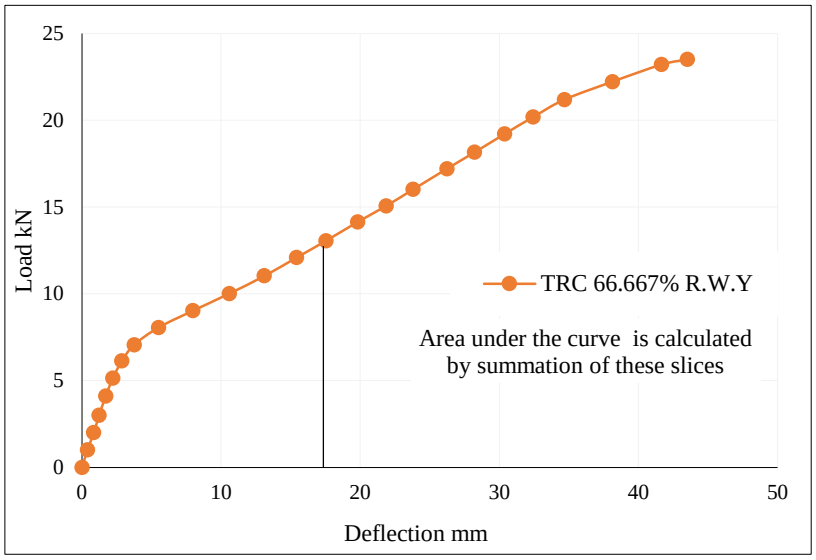

a) Toughness of the TRC 67% R.W.Y tested slab calculation by Method 1

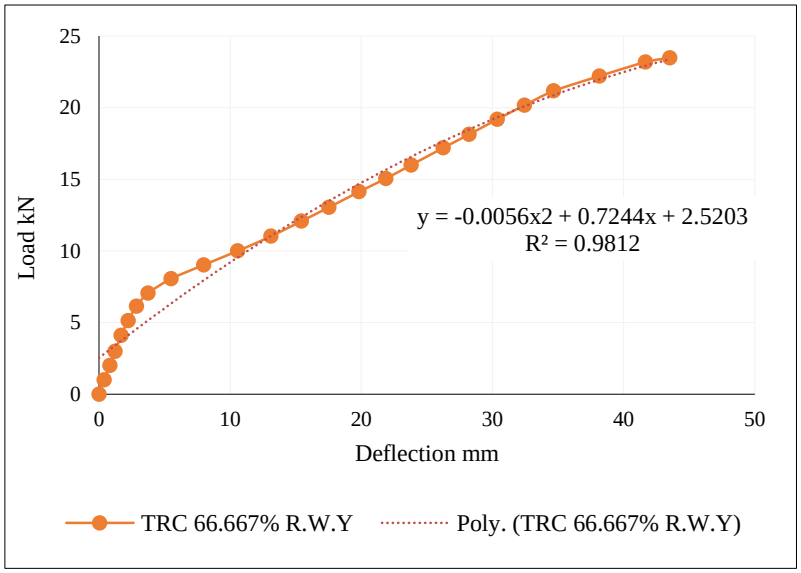

b) curve fitting for the TRC 67% R.W.Y tested slab

Figure 15. shows the two methods of the Toughness calculation

Figure 16 shows the toughness of the four TRC tested one way slabs. it can be noticed that the toughness is increased with the removing of the weft yarns by about 31.5%, 34.5% and 11.5% for the (TRC 50% R.W.Y, TRC 67% R.W.Y and TRC 75% R.W.Y) respectively in comparison with the (TRC 8L) this is imputed to the higher deflection that the (TRC 50% R.W.Y) yield with the same load that the two other removing specimens yield the lower mid-span deflection. However, the removing with the higher percent shows the lower toughness improvement this is accounted to the high exploitation of the yarn filaments hence the slippage is inhibited and the deflection decreased

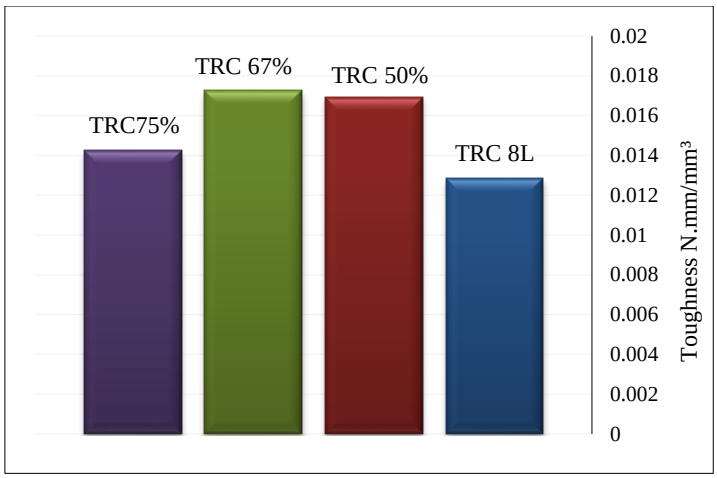

Figure 16. Show the Toughness for the four tested slabs

4.6. Ductility of the Four Tested TRC one, Way Slabs

The material ductility can be defined as the capacity to incur deformations without intrinsic decrease in the flexural capacity. The reinforced concrete flexural members' ductility can be expressed in the section ductility (curvature ductility) and member ductility:

$$\text{Section Ductility} = \frac{\emptyset u}{\emptyset y} \quad (1)$$

Where:

Øu is the curvature at the ultimate stage when the concrete strain attains its ultimate compression value.

Øy is the curvature when the tension reinforcement first reaches the yield strength.

$$Member\ Ductility = \frac{\Delta u}{\Delta y} \quad (2)$$

Where:

Δu is the mid span deflection at ultimate load, and Δy is mid span deflection at yield steel.

However, the clear yielding state of the textile reinforcements does not occur because of the filaments brittle failure characteristics. However, the deformability suggested method that accounted the effect of both strength and deflection factors on the ductility. The strength factor represents the ratio of the ultimate load to the load of 0.001 concrete compressive strain and the deflection factor is the ratio of the ultimate mid span deflection to member mid span deflection at the concrete strain. However, the 0.001 concrete strain represents the inception of the concrete inelastic deformation. The deformability factor must be exceeding the value of 4 according to the Canadian Standards Association (2012) (CAN/ CSA S-806 12) [19]. The deformability factor is calculated as follows:

$$Deformability\ Factor = Strength\ Factor \times Deflection\ Factor$$

$$Strength\ Factor = \frac{\text{Pu}}{\text{P0.001}} \quad \text{and} \quad Deflection\ Factor = \frac{\Delta u}{\Delta 0.001} \quad (3)$$

Table 8 illustrates the ductility values of the four tested slabs. The ductility increased by about 42%, 18.4% and 5.4% with the removing by 50%, 67% and 75% respectively as compared with the (TRC 8L) the superior mid span deflection of The (TRC 50% R.W.Y) leads to the higher ductility however the ductility enhancement is immediately descended with 67% and 75% of removing this is accounted to the enhancement of the interfacial bond between the concrete matrix and the textile reinforcement hence the filaments slippage is perfectly diminished. Figure 17 clarifies the ductility for the four TRC tested slabs.

Table 8. Ductility of the tested one, way slabs by two methods

Slab symbol	Strength factor	Deflection factor	Ductility
TRC 8L	1.93	2.78	5.37
TRC50%R.W.Y	2.51	3.69	9.26
TRC67%R.W.Y	2.13	3.32	7.07
TRC75%R.W.Y	2	2.71	5.42

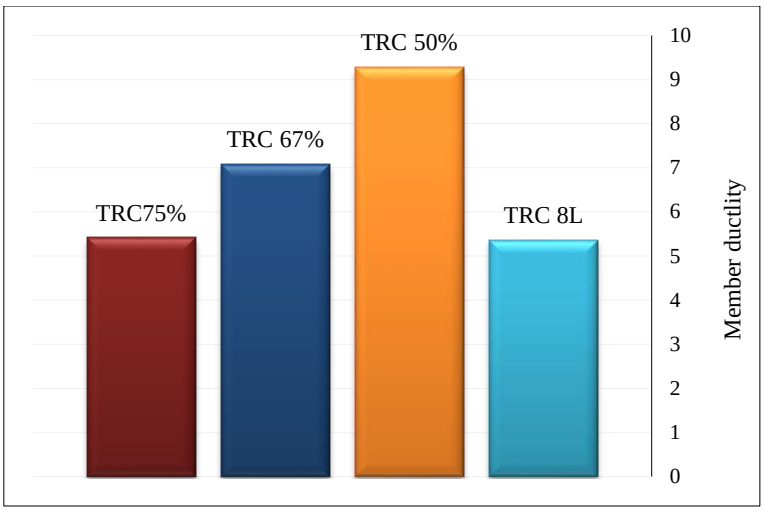

Figure 17. Show the Ductility for the four tested slabs

5. Design Method and Failure Criteria

5.1. Design Method

The TRCs growing usage in the past years has guided to a proper necessity to promote recent designing methods for the structural members that be content with requirements. Hegger et al. (2006) stated the non-availability of the design method or TRCs at present [20]. Thus the implementations of TRCs are though restricted. However, (Swamy and Mangat 1974) reported the main similarity between the conventional steel reinforced concrete and the continuous fiber reinforced concrete [21]. But (Voss 2006) stated that the TRCs behavior is differ from that of steel reinforced concrete this differences demonstrated in the textile material properties and bond characteristic [22]. The textile reinforcement load bearing capacity can indicate the flexural capacity of TRCs structural member. Thus the flexural capacity determination of the TRC member can be achieved by knowing the textile reinforcement tensile strength such as the steel reinforced concrete analogy [23, 24]. Alrshoudi (2015) suggested a design methodology to calculate the nominal bending capacity of TRC beam. He demonstrates the possibility of use the steel reinforced concrete design codes with take in to account the variations between the textile reinforcement and steel in term of bond behavior and yielding point [9]. The nominal bending moment of a TRC section can be calculated as follows:

$$M_n = \eta_\tau \rho_f b d^2 f_{fu} \left(1 - 0.59 \frac{\eta\tau\, \rho f \mathrm{fu}}{f'c}\right) \quad (4)$$

Where:

M_n is the nominal bending capacity.

η_τ is the bond efficiency factor.

ρ_f is the fabric reinforcement ratio.

f_{fu} is the ultimate tensile strength of the fabric.

$f'c$ is the compressive strength of concrete cylinder.

b is the width of the cross section.

d is the effective depth of the textile reinforcements.

The bond efficiency factor in this study was calculated for the four tested slabs by equalling the nominal bending moment with the experimental moment that obtained from the four-point bending test.

5.2. Failure Criteria

The failure pattern for the four tested one way slabs was the tensile failure in a ductile flexural mode when the most of the longitudinal carbon yarns were completely or partially ruptured since its tensile strain attaining the critical tensile strain. The four tested one way slabs fail with the telescopic failure which is defined by full rupture of the yarn sleeve filaments and sliding of the internal core filaments. As its observed the textile reinforcements bears the stresses after the first crack occurrence. The longitudinal textile reinforcements convert the stresses from the cracked concrete zone to the next un cracked concrete zone in a continuous gradual system till the failure. The significant tension stiffening effect of the textile reinforcements is perfectly observed since the cracks ascending is restricted by reducing the concrete strain at the cracks tips and the cracks propagation and distribution is quite controlled. The initiation of the newest micro

cracks in the zones between the two previous cracks confirmed the tension stiffening affect. Moreover, the friction at the longitudinal junctions that caused by the weft yarns may negatively affect the post cracking stiffness. At the final stage of loading no more recent cracks are created and the width of the main crack start to increase immediately thereafter the failure take place.

The textile reinforcement materials are un like the conventional steel reinforcement in an essential difference which is the plastic deformation, the steel reinforcements deform plastically after the yield while the textile reinforcement is bounded by linear elastic stage. However, the tensile strength of the textile reinforcements is more than that of steel reinforcements besides other considerations that mentioned previously which considered essential differences that differentiates the textile reinforcements rather than conventional steel reinforcements.

6. Conclusions

- The removing of the weft yarns improves the overall behavior of the TRC structural members in term of increasing the ultimate flexural capacity, ascends the compression concrete strain since the matrix performance is improved by enhancing the penetration through the layer openings.
- There is an optimal percent of removing that leads to increase the first crack stress, ultimate flexural strength, post cracking stiffness, toughness, reduce the ultimate deflection and yields higher number of cracks with the lower crack width.
- The TRC mechanical behavior is perfectly affecting by the interfacial bond between the textile reinforcements and the concrete matrix hence the removing of such nonstructural cross yarns can decrease the fibers content in the matrix and reduce the textile reinforcements congestion then the bond is improved.
- Enhancing the interfacial bond in such way enable the better exploitation of the yarn filaments which on the other hand is perfectly contributing in bearing the stresses and in the yarn stiffness.
- The removing of the weft yarns is perfectly reduced the volumetric ratio of the textile reinforcements however several studies account on improving the TRC overall behavior by the addition of the chopped fibers which is increases the volume of fibers content and the matrix compaction is certainly required in such case.
- Removing of the weft yarns with the higher percentage can reduce the cost of the textile reinforcements production.

7. Conflicts of Interest

The author declares no conflicts of interest.

8. Acknowledgments

The author would like to thank the staff of structural laboratory of the civil department in the college of Engineering at Diyala University-IRAQ for their assistance.

9. References

[1] Qinhua Li, and Shilang Xu. "Experimental Research on Mechanical Performance of Hybrid Fiber Reinforced Cementitious Composites with Polyvinyl Alcohol Short Fiber and Carbon Textile." Journal of Composite Materials 45, no. 1 (September 3, 2010): 5–28. doi:10.1177/0021998310371529.

[2] Zeweben, C. "Delaware Composites Design Encylopedia in Six Volumes Plus Index." Composites Science and Technology 42, no. 4 (January 1991): 429–432. doi:10.1016/0266-3538(91)90067-y.

[3] Bentur, A. and S. Mindess. "Fibre Reinforced Cementitious Composites, Second Edition" (November 22, 2006). doi:10.4324/9780203088722..

[4] Papanicolaou, Catherine G., and Ioannis C. Papantoniou. "Mechanical Behavior of Textile Reinforced Concrete (TRC) / Concrete Composite Elements." Journal of Advanced Concrete Technology 8, no. 1 (2010): 35–47. doi:10.3151/jact.8.35.

[5] Cohen, Zvi, and Alva Peled. "Controlled Telescopic Reinforcement System of Fabric–cement Composites — Durability Concerns." Cement and Concrete Research 40, no. 10 (October 2010): 1495–1506. doi:10.1016/j.cemconres.2010.06.003.

[6] Peled, A., and B. Mobasher. "Tensile Behavior of Fabric Cement-Based Composites: Pultruded and Cast." Journal of Materials in Civil Engineering 19, no. 4 (April 2007): 340–348. doi:10.1061/(asce)0899-1561(2007)19:4(340).

[7] Dvorkin, D., and A. Peled. "Effect of Reinforcement with Carbon Fabrics Impregnated with Nanoparticles on the Tensile Behavior of Cement-Based Composites." Cement and Concrete Research 85 (July 2016): 28–38. doi:10.1016/j.cemconres.2016.03.008.

[8] Dolatabadi, Mehdi Kamali, Steffen Janetzko, Thomas Gries, Bong-Gu Kang, and Andreas Sander. "Permeability of AR-Glass Fibers Roving Embedded in Cementitious Matrix." Materials and Structures 44, no. 1 (April 29, 2010): 245–251. doi:10.1617/s11527-010-9623-7.

[9] Alrshoudi, Fahed Abdullah S. "Textile Reinforced Concrete: Design Methodology and Novel Reinforcement." PhD diss., University of Leeds, 2015.

[10] Peled, Alva, Barzin Mobasher, and Arnon Bentur. "Textile Reinforced Concrete." Modern Concrete Technology (August 24, 2017). doi:10.1201/9781315119151.

[11] Peled, A., A. Bentur, and D. Yankelevsky. "Woven Fabric Reinforcement of Cement Matrix." Advanced Cement Based Materials 1, no. 5 (July 1994): 216–223. doi:10.1016/1065-7355(94)90027-2.

[12] Peled, A., A. Bentur, and D. Yankelevsky. "Flexural Performance of Cementitious Composites Reinforced with Woven Fabrics." Journal of Materials in Civil Engineering 11, no. 4 (November 1999): 325–330. doi:10.1061/(asce)0899-1561(1999)11:4(325).

[13] Colombo, Isabella Giorgia, Anna Magri, Giulio Zani, Matteo Colombo, and Marco di Prisco. "Erratum to: Textile Reinforced Concrete: Experimental Investigation on Design Parameters." Materials and Structures 46, no. 11 (April 4, 2013): 1953–1971. doi:10.1617/s11527-013-0023-7.

[14] Ghane, Mohammad, and Vahid Zarezadeh Lari. "Estimating the deflection of weft yarn in plain woven fabric using yarn pull out test." Indian Journal of Fibre & Textile Research (IJFTR) 39, no. 4 (2014): 394-400.

[15] Ortlepp, Regine. "Efficient Adaptive Test Method for Textile Development Length in TRC." Advances in Civil Engineering 2018 (July 15, 2018): 1–14. doi:10.1155/2018/4650102.

[16] ASTM C-494/C-494M. Standard Specification for Chemical Admixtures for Concrete. American Society for Testing and Materials. (2015).

[17] Yin, Shi-ping, Heng-lin Lü, and Shi-lang Xu. "Properties and Calculation of Normal Section Bearing Capacity of RC Flexural Beam with Skin Textile Reinforcement." Journal of Central South University 20, no. 6 (June 2013): 1731–1741. doi:10.1007/s11771-013-1666-9.

[18] Du, Yunxing, Xinying Zhang, Lingling Liu, Fen Zhou, Deju Zhu, and Wei Pan. "Flexural Behaviour of Carbon Textile-Reinforced Concrete with Prestress and Steel Fibres." Polymers 10, no. 1 (January 20, 2018): 98. doi:10.3390/polym10010098.

[19] Canadian Standards Association (CAN/ CSA S-806 12). Design and construction of building structures with fiber reinforced polymers. Canadian Standards Association, Canada, (2012).

[20] Hegger, J., N. Will, O. Bruckermann, and S. Voss. "Load–bearing Behaviour and Simulation of Textile Reinforced Concrete." Materials and Structures 39, no. 8 (July 19, 2006): 765–776. doi:10.1617/s11527-005-9039-y.

[21] Swamy, R.N., and P.S. Mangat. "A Theory for the Flexural Strength of Steel Fiber Reinforced Concrete." Cement and Concrete Research 4, no. 2 (March 1974): 313–325. doi:10.1016/0008-8846(74)90142-2.

[22] Voss, S. DESIGN METHODS FOR TEXTILE REINFORCED CONCRETE. In: T. VOGEL, N. MOJSILOVIĆ and P. MARTI, eds. 6th International PhD Symposium in Civil Engineering, August 23-26, 2006, Zurich.

[23] Brameshuber, W. and T. Brockmann. Introduction. In: W. BRAMESHUBER, ed. Textile Reinforced Concrete - State-of-the-Art Report of RILEM TC 201-TRC. RILEM Publications SARL. (2006).

[24] Voss, S. "Dimensioning of Textile Reinforced Concrete Structures." ICTRC'2006 - 1st International RILEM Conference on Textile Reinforced Concrete (2006). doi:10.1617/2351580087.015.